

Scaling up the Production Rate of Nanofibers by Needleless Electrospinning from Multiple Ring

Xin Wang^{1,2*}, Tong Lin², and Xungai Wang^{1,2}

¹*School of Textile Science and Engineering, Wuhan Textile University, Wuhan 430200, China*

²*Australian Future Fibres Research and Innovation Centre, Deakin University, Geelong 3217, Australia*

(Received August 16, 2013; Revised October 8, 2013; Accepted October 20, 2013)

Abstract: Mass production of nanofibers is crucial in both laboratory research and industry application of nanofibers. In this study, multiple ring spinnerets have been used to generate needleless electrospinning. Multiple polymer jets were produced from the top of each ring in the spinning process, resulting in thin and uniform nanofibers. Production rate of nanofibers increased gradually with the increase of the number of rings in the spinneret. Spinning performance of multiple ring electrospinning, namely the quality and production rate of the as-spun nanofibers, was dependent on experimental parameters like applied voltage and polymer concentration. Electric field analysis of multiple ring showed that high concentrated electric field was formed on the surface of each ring. Fiber diameter together with production rate of needleless electrospinning was dependent on the strength and distribution of the electric field of the spinneret. Needleless electrospinning from multiple ring can be further applied in both laboratory research and industry where large amount of nanofibers must be employed simultaneously.

Keywords: Needleless electrospinning, Ring, Nanofiber, Electric field analysis

Introduction

Nanofiber has been a research focus since 1990s due to its application potential in diverse areas [1,2]. Electrospinning is regarded as the most widely used method in producing nanofibers due to its simplicity, effectiveness and applicability to different kinds of polymers available in today's industry market [3]. However, a realizable electrospinning technique with the ability to produce uniform nanofibers on large scale is still of great challenge. In this regard, efforts have been putting on the optimization and development of existing electrospinning techniques [4-6]. In order to enhance the productivity and uniformity of the as-spun nanofibers, multiple polymer jets must be drawn out from the spinneret at the same time and the applied voltage must be high enough to generate strong electric field around the spinneret. For conventional needle electrospinning, high electric field can be easily generated on the tip of the needle, but limited polymer jets can be produced from the needle in the spinning process which leads to a very low production rate of nanofibers. Needleless electrospinning was developed to produce nanofibers from a much larger surface than needle electrospinning so that the production rate was increased greatly [7]. For this purpose, previous study on needleless electrospinning was focused on the modification of the geometry of spinneret. Spinnerets made of cylinder/wired cylindrical electrode [8,9], disc [10], coil [11,12], cone [13], tube [14,15], and slit [16] were successfully developed. On the other hand, the quality of nanofibers, such as the diameter and its distribution and surface morphology, can be controlled by modifying the present electrospinning system [17,18].

Theoretically, spinnerets with different geometries could be applied in needleless electrospinning, but how to concentrate the electric field around the spinneret so as to initiate the spinning process is an important issue. Generation of multiple polymer jets in needleless electrospinning has been explained to be resulted from electrically amplified liquid waves [15]. The jet formation in needleless electrospinning is greatly dependent on the external electric field and other related experimental parameters. As electric field is usually concentrated around the spinneret, the geometry of spinnerets is the key factor that affects the distribution of electric field and thus the spinning process and the quality of the as-spun nanofibers [11]. There is no direct method to measure the electric field in electrospinning as high voltage involved in the process hampers the testing. However, finite element method (FEM) has been successfully applied to model the electric field profile and intensity of spinnerets of needleless electrospinning [19]. It provides an indirect way to characterize the electric field in needleless electrospinning which further contributes to the understanding of the spinning mechanism and optimal designing of spinnerets.

Previously, a comparative study on cylinder and disc electrospinning showed that disc had higher efficiency in concentrating electric field so as to generate needleless electrospinning [9]. However, a more efficient spinneret with delicate geometry is still needed for exploration of needleless electrospinning so that lower energy usage and thinner fibers and finally higher fiber production rate could be achieved. Later on, wire coil structure was used to generate needleless electrospinning, it produced much thinner fibers due to a more highly concentrated electric field it exhibited [11,12]. In order to further optimize needleless electrospinning and scale up the production rate of nanofibers, ring structure

*Corresponding author: wangxin0222@hotmail.com

was used in this study to generate needleless electrospinning. This setup showed high production rate of thin and uniform nanofibers, it can be easily scaled up to desired extent by employing more rings in spinneret. Needleless electrospinning using multiple ring can be widely applied in both laboratory research and industry production of nanofibers.

Experimental

Materials

PVA (average molecular weight 146,000-186,000, 96 % hydrolyzed), obtained from Aldrich-Sigma, was used as the model polymer. PVA solutions (with different wt%) were prepared by dissolving the PVA powder in deionized water at 90 °C, with intensive stirring for about 12 h and without adding any additives in the solution.

Needleless Electrospinning

The apparatus for the needleless electrospinning from multiple ring structures is depicted in Figure 1(a). A rotating ring made from copper wire was used to pick up polymer solution from the polymer reservoir; the rotating speed was set as 40 rpm. The ring shape was set as length=16 cm; ring diameter=8 cm and wire diameter=2 mm. Alternatively,

multiple ring (pitch=4 cm) were also used as spinneret to generate needleless electrospinning, as shown in Figure 1(a). The polymer solution was connected to a high voltage power supply (ES100P, Gamma High Voltage Research) via an inserted electrode in the reservoir; conventional applied voltage was set as 60 kV. An aluminium plate was used to collect the nanofibers with a collecting distance of 13 cm. The spinning process was conducted in standard ambient conditions with temperature 20 ± 3 °C and relative humidity 65 ± 5 %.

Characterizations and Measurements

The fiber morphology was observed under a scanning electron microscope (SEM, Leica S440). The average fiber diameter was calculated from the SEM photos with the aid of image analysis software (ImagePro+4.5), more than 100 fibers were tested from at least four SEM photos that were taken from different areas of a given sample, results were averaged and the standard deviation was calculated to show the diameter distribution range. Production rate was tested by weighing the collected fibers in every 10 min.

The electric field profile of different electrospinning setups was modeled using a finite element analysis (COMSOL 3.5a) [20]. In a typical process for analysis of electric field

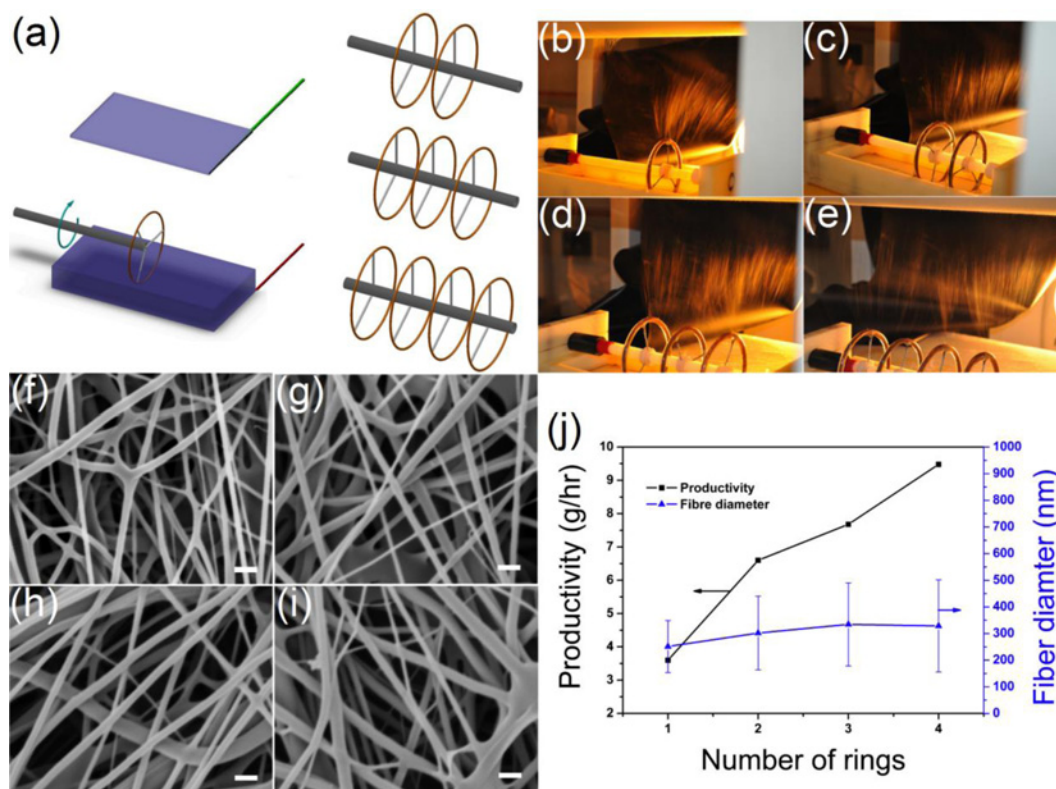


Figure 1. Needleless electrospinning from ring/multiple ring spinnerets. (a) Schematic of the setup and spinnerets, (b-e) Photos of spinning process using spinnerets with different number of rings, (f-i) SEM photos of the as-spun nanofibers using spinnerets with ring number of one, two, three and four, respectively (bar=1 μ m), (j) Production rate and fiber diameter of needleless electrospinning using spinnerets with different number of rings (Applied voltage=60 kV; PVA concentration=9 %).

of needleless electrospinning, the ring spinneret (length=16 cm; ring diameter=8 cm and wire diameter=2 mm) was first defined using *SOLIDWORKS*, and a bi-interface was used to transfer the defined geometry into the *COMSOL* interface. Other parts such as plate collector (24 cm long, 15 cm wide and 5 mm thick) and bath (24 cm in length, 10 cm in width and 4 cm in height) could then be drawn directly in *COMSOL*. After setting the sub-domain and boundary, the meshing process could be performed and finally the electric field intensity profile could be solved. The electric field intensity was calculated at the same time from the modeled electric field profiles.

Results and Discussion

Needleless electrospinning was successfully generated from multiple ring spinnerets. As illustrated in Figure 1(a), multiple ring spinnerets were used as the fiber generator which was partly immersed (roughly one third of the ring) in the polymer bath so as to make polymer solution coated on its surface by rotating. The viscoelastic nature of the polymer solution assisted in the formation of an evenly distributed solution layer on each ring. When the rings together with polymer solution were charged with an electric voltage of 60 kV, multiple polymer jets were formed from the surface of each ring, as shown in Figure 1(b)-(e). The numerous polymer jets were clearly observed from a circular sector zone with a central angle of about 90 degree in the top sector of each ring.

The as-spun nanofibers show nanofibrous morphology without beads-in-string structure, as shown in Figure 1(f)-(i). The diameter of the nanofibers is less than 1 μm and the most of the fibers are isolated from each other. Some fibers stick to each other forming an inter-connected fibrous structure. The reason for the formation of bonded fibrous structure is because of the insufficient evaporation of solvent (water) from the polymer jets. This is usually the case for electrospinning from PVA, especially when numerous jets have been generated simultaneously in a very limited space during needleless electrospinning. The photos from spinnerets with different number of rings show similar morphology as seen from Figure 1(f)-(i), except that many coarse fibers can be observed when more than one ring has been used. Statistic analysis of the fiber diameter has been conducted based on SEM photos and the results are shown in Figure 1(j). It is evident that with the increase of the number of rings, the average diameter of collected nanofibers increases slightly, so as the standard deviation. This may be ascribed to the emerging of coarse fibers as shown from SEM photos in Figure 1(g)-(i). This suggests that fibers produced from single ring are more uniform and thinner.

The production rate of nanofibers increases with the increase of the number of rings. The setup using single ring could yield nanofibers of 3.5 g/hr under applied voltage of

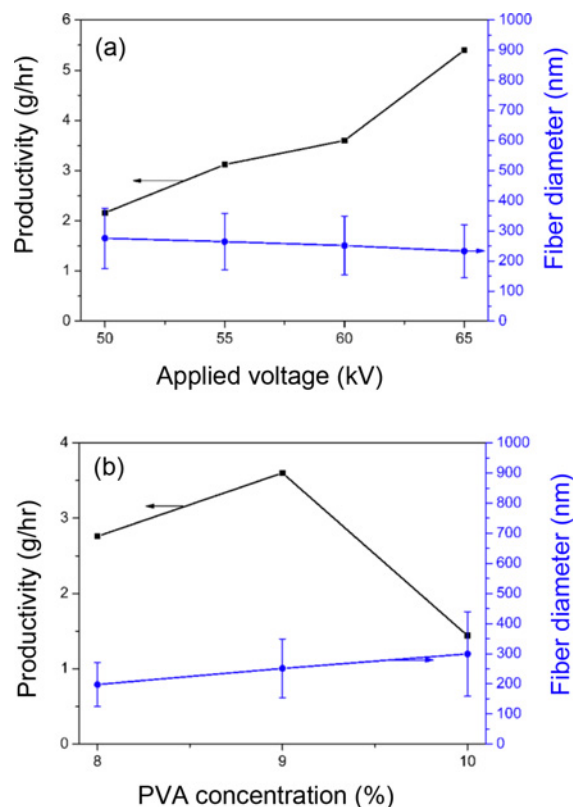


Figure 2. Effect of applied voltage (a) and PVA concentration (b) on the production rate and fiber diameter of needleless electrospinning from single ring.

60 kV, the production rate of two rings increased to around 6.6 g/hr. Further increase of the number of rings results in gradual increase (but not in linear manner) of production rate as shown in Figure 1(j). The increase of production rate is due to the increase of polymer jets with the increase of the number of rings, as shown in Figure 1(b)-(e). As a whole, increasing the number of rings can scale up the production rate of nanofibers. Considering the production rate of conventional needle electrospinning is less than 0.3 g/hr [10], needleless electrospinning from multiple ring has enhanced the production rate of nanofibers to a much higher level. In order to commercialize needleless electrospinning, the spinneret needs to be long and efficient enough to produce sufficient nanofibers in a short time to match the industrial requirements. Single ring structure, however, is competent in laboratory research on large-scale production of nanofibers.

The generating of polymer jets was greatly influenced by the experimental parameters such as applied voltage and polymer concentration. The applied voltage was found to be a crucial parameter that decided the production rate and the quality of as-spun nanofibers. As shown in Figure 2(a), the fiber diameter decreases almost linearly with the increase of applied voltage, the standard deviation is slightly decreased at the same time suggesting that more uniform fibers were

produced. Stronger electric field is formed under higher applied voltage in needleless electrospinning thus higher electrostatic force will be applied to the coated polymer solution on the surface of the ring; the polymer jet will be attenuated more sufficiently so that the as-spun nanofibers are thinner and more uniform. Meanwhile, the production rate of nanofibers increases gradually with the increase of applied voltage, this can also be ascribed to the stronger electric field formed on the ring under higher applied voltage.

PVA solution with concentration in the range of 8-10 % was successfully electrospun on this needleless electrospinning setup. PVA solution with concentration lower than 8 % was unable to generate continuous spinning process, the collected products showed beads-on-string structure or even beads. While very coarse fibers were produced and the spinning process was inconsecutive when too high a PVA concentration, such as 11 %, was used. Owing to the high viscosity of polymer solution with high concentration, fiber diameter and the associated standard deviation increases with the increase of PVA concentration, as shown in Figure 2(b). At the same time, when PVA concentration was higher than 9 %, less polymer jets were produced due to the increased viscosity of the polymer solution. Thus the production rate drops suddenly when PVA concentration is higher than 9 %. Further increase of PVA concentration resulted in inconsecutive spinning process with extremely low production rate.

Electric field has been regarded as the dominant factor that determines the electrospinning performance [15,16]. Electric field profiles of needleless electrospinning system with different number of rings are shown in Figure 3(a)-(d). Strong electric field has been formed on the top area of each ring with intensity higher than 50 kV/cm. In physics, charge density on the surface of an irregularly shaped conductor is high in convex regions with a small radius of curvature, thus

the concentrated electric field is formed on the top of each ring. When the number of rings increases, it is evident that stronger electric field tends to form on both the side rings, while the electric field of the middle rings is relatively weaker. Figure 3(e) shows the electric field intensity along the spinning direction from the center to the top of the ring and then to the collector. The electric field intensity increases to its peak swiftly and then drops suddenly to almost zero; the intensity peak appears at the top of each ring. The intensity values show the overall intensity decreases with the increase of the number of the rings and the intensity of the middle rings is lower than that of the side rings.

The evolvement of electric field of multiple ring spinnerets in Figure 3 can be applied to explain the trend of fiber diameter and production rate in Figure 1. The overall electric field intensity decreases with the increase of the number of rings, which led to the larger fiber diameter due to lower electrostatic force. Besides, the differences in electric field intensity between each ring in multiple ring spinneret result in different values of electrostatic force on the top of each ring; this incurs uneven fibers with relatively high standard deviation. On the other hand, the intensity of each ring in multiple ring spinnerets is high enough to generate needleless electrospinning, increase of the number of rings in spinneret means that more rings have been employed as fiber generator, so that the overall production rate increases accordingly. But the production rate doesn't show linear relation with the number of rings, this is due to the different spinnability of each ring in the multiple ring spinnerets. The side rings may produce more polymer jets than the middle rings due to the stronger electric field of the side rings. Thus the overall production rate was lower than the calculated product of the number of rings and the production rate of single ring. It was noted that the geometry of the multiple ring electrode

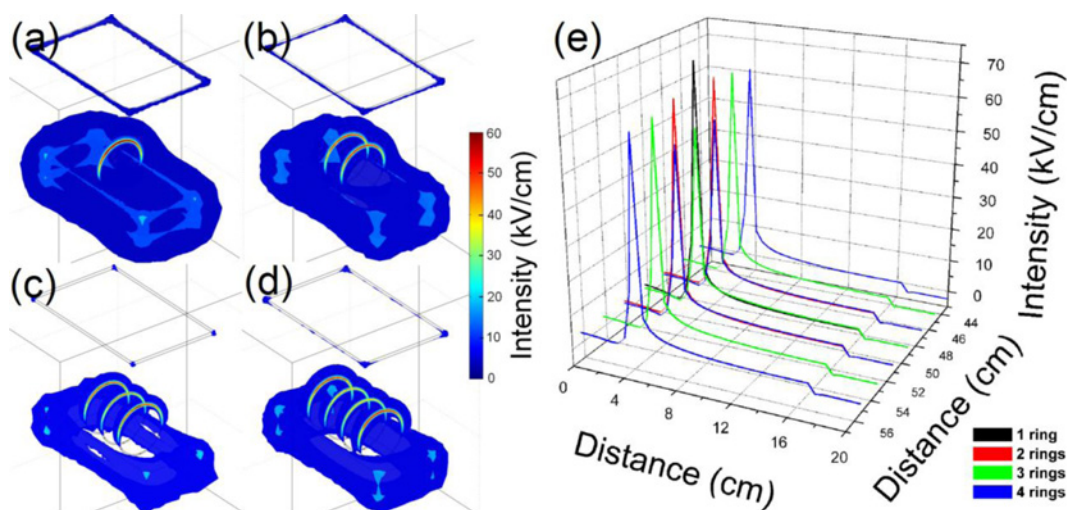


Figure 3. Electric field analysis of needleless electrospinning from multiple ring; (a-d) electric field profiles with the number of rings one, two, three and four, respectively, and (e) electric field intensity along the spinning direction.

affected the generation needleless electrospinning. A proper distance (larger than 1 cm and smaller than 8 cm) between neighboring rings is applicable to avoid interferences between rings and non-uniform collection of nanofibers.

Needleless electrospinning from multiple ring spinnerets will provide laboratory prototype for research in electrospinning that shows great potential in mass production of nanofiber production as the number of rings in the spinneret can scale up to increase production rate to a satisfied level. It shows great potential in industry production of nanofibers subject to the possibility of scaling up the spinnerets to desired level. It also provides probability in producing mixed and composite nanofibers as each ring in the spinneret can be fed with different polymer materials.

Conclusion

Multiple ring structure was successfully applied to generate needleless electrospinning. Multiple polymer jets were produced from the top area of each ring of the spinneret. SEM photos of the as-spun nanofibers showed that thin and uniform nanofibers without beads were produced. Production rate of nanofibers was much higher than that of needle electrospinning, and it could be scaled up with the increase of the number of rings in the spinneret. More uniform nanofibers were produced as the applied voltage increased, the production rate increased at the same time owing to the increased electrostatic force in the spinning process. Fiber diameter increased with the increase of PVA concentration and spinning process was incontinuous when the concentration was higher than 10%. Electric field analysis of multiple ring spinnerets showed high concentrated electric field formed on the top of each ring. Fiber diameter together with production rate of needleless electrospinning was dependent on the electric field profile and intensity of the spinnerets.

Acknowledgments

Funding supports from National Natural Science Foundation of China (Grant No. 51103109), Education Bureau of Hubei Province, China (Grant No. D20121710), Department of Science and Technology of Hubei Province, China (Project No. 2012FFB04606) and Research Funding from Wuhan

Textile University, China are greatly appreciated.

References

1. A. Greiner and J. H. Wendorff, *Angew. Chem. Int. Edit.*, **46**, 5670 (2007).
2. D. Li and Y. Xia, *Adv. Mater.*, **16**, 1151 (2004).
3. D. H. Reneker and I. Chun, *Nanotechnology*, **7**, 216 (1996).
4. B. Ding, E. Kimura, T. Sato, S. Fujita, and S. Shiratori, *Polymer*, **45**, 1895 (2004).
5. G. Kim, Y. S. Cho, and W. D. Kim, *Eur. Polym. J.*, **42**, 2031 (2006).
6. W. E. Teo and S. Ramakrishna, *Nanotechnology*, **17**, R89 (2006).
7. A. L. Yarin and E. Zussman, *Polymer*, **45**, 2977 (2004).
8. O. Jirsak, F. Sanetnik, D. Lukas, V. Kotek, L. Martinova, and J. Chaloupek, Patent, WO 2005/024101 A1 (2005).
9. D. Petras, M. Maly, J. Pozner, J. Trdlicka, and M. Kovac, Patent, WO 2008/028428 A1 (2008).
10. H. Niu, T. Lin, and X. Wang, *J. Appl. Polym. Sci.*, **114**, 3524 (2009).
11. X. Wang, H. Niu, T. Lin, and X. Wang, *Polym. Eng. Sci.*, **49**, 1582 (2009).
12. X. Wang, H. Niu, X. Wang, and T. Lin, *J. Nanomater.*, **2012**, 785920 (2012).
13. B. Lu, Y. Wang, Y. Liu, H. Duan, J. Zhou, Z. Zhang, W. Youqing, X. Li, W. Wang, W. Lan, and E. Xie, *Small*, **6**, 1612 (2010).
14. O. O. Dosunmu, G. G. Chase, W. Kataphinan, and D. H. Reneker, *Nanotechnology*, **17**, 1123 (2006).
15. J. S. Varabhas, G. G. Chase, and D. H. Reneker, *Polymer*, **49**, 4226 (2008).
16. D. Lukas, A. Sarkar, and P. Pokorny, *J. Appl. Phys.*, **103**, 084309 (2008).
17. D. G. Yu, J. H. Yu, L. Chen, G. R. Williams, and X. Wang, *Carbohydr. Polym.*, **90**, 1016 (2012).
18. D. G. Yu, C. Branford-White, S. W. Bligh, K. White, N. P. Chatterton, and L. M. Zhu, *Macromol. Rapid. Commun.*, **32**, 744 (2011).
19. X. Wang, X. Wang, and T. Lin, *J. Mater. Res.*, **27**, 3013 (2012).
20. X. Wang, X. Wang, and T. Lin, *J. Ind. Text.*, DOI: 10.1177/1528083713498916.